

Econometric vs. Causal Structure-Learning for Time-Series Policy Decisions: Evidence from the UK COVID-19 Policies

Bruno Petrongaro^{1*} and Anthony C. Constantinou¹

^{1*}Bayesian Artificial Intelligence research lab, MInDS research group, School of Electronic Engineering and Computer Science, Queen Mary University of London, Mile End Road, London, E1 4NS, UK.

*Corresponding author(s). E-mail(s): b.petrongaro@qmul.ac.uk;
Contributing authors: a.constantinou@qmul.ac.uk;

Abstract

Causal machine learning (ML) recovers graphical structures that inform us about potential cause-and-effect relationships. Most progress has focused on cross-sectional data with no explicit time order, whereas recovering causal structures from time series data remains the subject of ongoing research in causal ML. In addition to traditional causal ML, such as score-based and constraint-based algorithms, this study assesses econometric methods that some argue can recover causal structures from time series data. They have been used for such purposes in economics, biology and other fields. The use of these methods can be explained by the significant attention the field of econometrics has given to causality, and specifically to time series, over the years. This presents the possibility of comparing the causal discovery performance between econometric and traditional causal ML algorithms. We seek to understand if there are lessons to be incorporated into causal ML from econometrics, and provide code to translate the results of these econometric methods to the most widely-used Bayesian Network R library, `bnlearn`. We investigate the benefits and challenges that these algorithms present in supporting policy decision-making, using the real-world case of COVID-19 in the UK as an example. Four econometric methods are evaluated in terms of graphical structure, model dimensionality, and their ability to recover causal effects, and these results are compared with those of eleven causal ML algorithms. Amongst our main results, we see that score-based causal-ML methods often recover more identifiable effects, but typically via much denser graphs. Methodologies based on the idea of shrinkage can surface plausible intervention targets, yet no single class dominates across all metrics. Overall, the evaluation

suggests complementary strengths. Econometric methods provide clear rules for temporal structures, whereas causal-ML algorithms offer broader discovery by exploring a larger space of graph structures that tends to lead to denser graphs that capture more identifiable causal relationships.

Keywords: Directed acyclic graphs, structure learning, time-series, causal inference, model averaging, COVID-19

1 Introduction

Focusing on associations can be misleading for policy design and evaluation; we need to determine if changes in one variable cause changes in another. Traditional Machine Learning (ML) models are unsuitable for answering this question, as they focus on associations and cannot simulate the impact of hypothetical actions to inform decision-making. One must rely on influential or causal assumptions that these models do not capture.

Causal Machine Learning (Causal ML) focuses on unsupervised learning algorithms that aim to recover causal relationships from both observational and interventional data. In this study, causal ML refers specifically to causal structure learning algorithms, which focus on learning dependency structure amongst available variables, with additional causal assumptions required to interpret that structure as a causal model. This can be thought of as a map of cause-and-effect relationships of these variables. The two traditional classes of structure learning algorithms are score-based and constraint-based algorithms. Score-based learning focuses on searching the space of possible structures and optimising a score that reflects how well the learnt structure fits the data, whereas constraint-based learning uses conditional independence tests to infer causal structures. Hybrid algorithms that combine these two classes of learning are often viewed as a third class of structure learning.

Over the past few decades, there have been substantial methodological improvements in causal structure learning algorithms. However, their real-world impact remains more limited than that of traditional associational ML approaches. This is because discovering causal relationships from observational data remains extremely difficult and, unlike associational ML, small errors in causal discovery can lead to large negative repercussions in causal inference. This might explain why the literature on policy recommendations remains predominantly from the field of econometrics. That is, while other fields have undoubtedly contributed to developments in optimal decision-making, economics remains one of the most deeply engaged disciplines in these topics.

[1] is an excellent example of a widely influential discussion on methodological approaches in econometrics that favours research designs that resemble Randomised Controlled Trials (RCTs). However, [1] also mentions the developments in the ML field and their potential. Instrumental variables, regression discontinuity designs, and difference-in-differences methodologies remain the preferred tools for causal inference amongst econometricians. These methods have produced exciting work, such as

[2], which employs a regression discontinuity design to estimate the causal effect of immigrant legalisation on the crime rate of immigrants in Italy, concluding that legalisation reduces the crime rate of legalised immigrants. However, like Causal ML, these methods are not free of limitations. [1] summarises issues related to weak or flawed identification strategies and problems related to this analysis’s inability to generalise to other settings.

The limited development of Causal ML for time-series data presents a valuable opportunity to evaluate how well these methods support policy decisions in a real-world setting under such conditions, and to compare them with econometric techniques that are routinely used for that purpose. This study will address causality in time-series data, which adds a layer of complexity to this type of analysis. In the era of big data, massive amounts of data are continually generated over time, evolve with time and respond to external shocks, such as policy changes. The selected use case is COVID-19 in the UK, as described in detail in Section 3. Stating this as our objective implies that we will be evaluating the following:

- The ability of these econometric methods to recover cause-and-effect relationships from observational time-series data. This involves understanding how these methods perform in the most fundamental objective for Causal ML; i.e., recovering cause-and-effect relationships from observational data.
- The ability of the recovered model structure implied by these cause-and-effect relationships to identify and correctly estimate the direction of the causal effects; i.e., determining whether the effect increases or decreases.

2 Background

The development of Causal ML in the context of recovering cause-and-effect relationships from time-series data has been limited compared to econometrics. We were able to identify the following studies related to causal ML with time series data:

- [3] introduces two online causal structure learning algorithms: Online Fast Causal Inference (OFCI) and Fast Online Fast Causal Inference (FOFCI). OFCI is an online version of Fast Causal Inference (FCI) modified to handle latent variables and dynamic, time-changing causal structures. It works by revising correlations as new data points come in and then relearning the structure when the data indicates a significant change. FOFCI is a modification of OFCI designed to minimise learning costs and speed learning by utilising causal relationships learnt from previous models, while preserving model fit.
- [4] introduces DOCL, a causal structure learning algorithm that focuses on real-world environments where causal structures can change unpredictably. DOCL processes streaming data in real-time and adapts to changes in both causal structure and underlying probabilistic relationships learnt from sequential or ordered data.
- [5] developed the Local Stationarity Structure Tracking (LoSST) structure learning algorithm, which assumes local stationarity in the data generation process. LoSST dynamically tracks and adapts to changes in both the causal structure and relationships in real-time.

Although these studies are relevant, they aim to identify changes in causal structures. In contrast, we are interested in distribution shifts where the graph remains fixed but inputs, including seasonality, policy, behaviour-driven shifts, amongst others, alter observed distributions without implying new causal links.

Econometrics offers extensive time series approaches suitable for addressing this issue. A detailed explanation of how these methods can aid in recovering causal structures is provided in Section 4. However, it will become clear that the time-series analysis methods presented work similarly to traditional causal ML methods. This is because a non-significant coefficient suggests that, after controlling for the other variables in a model, no evidence for dependence between the predictor and the target was found. This outcome is consistent with the predictor and the target being conditionally independent. The idea is similar to conventional causal discovery methods, which test for conditional independence between variables. However, regression-based inference can sometimes reflect spurious associations if important confounders are omitted. Another econometric method used involves searching for network modules, which essentially means identifying groups of interrelated nodes. This is what methods that recover causal structures do.

After learning the structures, the models can be converted into Dynamic Bayesian Networks (DBNs). A DBN is a probabilistic graphical model specifically designed to represent variables and their dependencies across different points in time. Similar to a standard Bayesian Network (BN), a DBN represents variables as nodes and their dependencies as directed arcs via a Directed Acyclic Graph (DAG). However, unlike a standard BN, where each variable is represented by a single node, a DBN represents each variable using multiple nodes, each corresponding to the same variable at different points in time. Arcs in a DBN are drawn between variables at successive time points whenever these variables are not independent of the past variable after accounting for all other relevant past variables.

In terms of parameterisation, discrete BNs typically represent dependencies using Conditional Probability Tables (CPTs), while continuous BNs employ conditional probability distributions. Under certain assumptions, BNs or DBNs can be interpreted causally, transforming the DAG into a Causal Bayesian Network (CBN). CBNs are important to this study because they enable us to model the effect of hypothetical interventions and estimate their effects, therefore enabling optimal decision-making under uncertainty.

Despite their utility, most of the applied work on BNs has been targeted to cross-sectional data (data collected at one specific point in time across multiple entities), or it has assumed that the data has been generated from multiple independent realisations of a process (repeated cross-sectional data pooled together and treated as a cross-sectional dataset). This is because BN structure learning algorithms are usually not designed to capture the evolution of a system over time, the variables that compose this system, or how their interrelations change with time.

3 COVID-19 case study data

To evaluate the usefulness of these methods for supporting policy decisions, we have selected the debated policy responses to COVID-19. The COVID-19 pandemic, caused by the SARS-CoV-2 virus, posed significant public health and policy challenges globally.

For example, vaccines are typically regarded as the primary strategy for managing the spread of viral diseases, and this expectation carried over to COVID-19 once effective vaccines were developed. Other actions related to managing the spread of this disease were viewed by many as temporary measures until a vaccine became available. This may be because traditional models for infectious disease epidemics, inspired by [6], rely on the assumption that any member of the population can infect or be infected by any other. Many models disregard the actual interactions within a population and how diseases spread. However, it is most likely that this expectation persisted because the economic costs of implementing social distancing measures are high.

Since traditional models do not account for actual interactions within a population, and the cost of social distancing measures is high, the question arises: Which interventions are most effective in reducing the infection rate? COVID-19 will not be the last pandemic, so this crucial question is: since neither vaccines nor treatments will generally be readily available at the beginning of pandemics, can we utilise knowledge on ways to limit interactions within a population as a faster way to control pandemics? Modelling these effects by simulating hypothetical interventions in a causal inference framework [7] may help support decision-making in future pandemics.

We use routinely collected publicly available aggregated data, which was widely used during the pandemic in the UK. For a detailed description of how the data was collected, please refer to [8]. The additional relevant data collected for this study were obtained from the same sources as those cited in [8]. These are [9] and [10]. The dataset used in this study contains 46 columns and 866 rows, where each column corresponds to a variable and each data row to a daily outcome. The first column of the data refers to the time indicator, 'Date', which spans from January 30, 2020, to June 13, 2022. The dataset contains both continuous and categorical variables, as well as missing data values. Descriptions of the variables are provided in Table 1.

Table 1: The COVID-19 Dataset

Variable	Description
Date	Date observations were recorded.
Excess mortality (EM)	Percentage difference between reported and projected deaths.
Schools	Whether schools were open, partially open, or closed.
Face masks (FM)	Mask mandates during the pandemic: optional, mandatory, or no mandate.
Lockdown severity (LS)	Severity of lockdown: severe, moderate, weak, or limited measures/social distancing only.
Majority COVID-19 variant (Variant)	The majority COVID-19 variant.

Variable	Description (continued)
Flights 7-day moving average	7-day moving average of flights.
OpenTable restaurant (Restaurant)	OpenTable index on restaurant bookings in London.
Google homeworking (Homeworking)	Google index on homeworking in Greater London.
Google workplace (Workplace)	Google index on workplace activity in Greater London.
Apple walking (Walking)	Apple index on walking activity in London.
Google parks (Parks)	Google index on park visits in Greater London.
Google retail & recreation (Retail & recreation)	Google index on retail and recreation in Greater London.
Google grocery & pharmacy (Grocery & Pharmacy)	Google index on grocery and pharmacy in Greater London.
Google transit stations (Transit)	Google index on transit station activity.
TfL Tube (Tube)	TfL index on tube activity.
TfL Bus (Bus)	TfL index on bus activity.
Citymapper journeys (Journeys)	Citymapper index on journey activity.
Season	Winter, autumn, summer, and spring.
PCR tests	Number of tests on date.
PCR tests capacity	Capacity level on date.
Antibody tests	Number of tests on date.
Antibody tests capacity	Capacity level on date.
Pillar 1 capacity	NHS/UKHSA capacity on date.
Pillar 2 capacity	UK Government capacity on date.
Pillar 3 capacity	Antibody testing capacity on date.
Pillar 4 capacity	Surveillance testing capacity on date.
Pillar 1 tests	NHS/UKHSA tests on date.
Pillar 2 tests	UK Government tests on date.
Pillar 3 tests	Antibody tests on date.
Pillar 4 tests	Surveillance tests on date.
Tests across all 4 Pillars	Total tests on date.
New cases	People testing positive for COVID-19 on date.
New infections	New infections on date.
Reinfections	New reinfections on date.
Hospital admissions	Patients admitted to hospital with COVID-19.
Patients in hospital	Patients in hospital with COVID-19.
COVID-19 patients in MVBs	Patients in Mechanical Ventilator Beds (MVBs) with COVID-19.
Vaccinations (total)	Total vaccines administered on date.
Vaccinations (1st dose)	First dose vaccines administered on date.

Variable	Description (continued)
Vaccinations (2nd dose)	Second dose vaccines administered on date.
Vaccinations (3rd dose)	Third dose vaccines administered on date.
1st dose uptake	Reported first dose uptake.
2nd dose uptake	Reported second dose uptake.
3rd dose uptake	Reported third dose uptake.
COVID-19 deaths on certificate	Daily deaths with COVID-19 on certificate by date of death.

3.1 Data missingness and imputation

Out of a total of 46 variables in the dataset, 40 variables contain at least one missing value, corresponding to approximately 86.96% of all variables. Overall, there are 5,667 missing values, representing 14.23% of the data values. Table 2 offers a summary of missing data per variable. Key information includes:

- Vaccination data (especially the 3rd dose variables) show the highest proportion of missing values, ranging from approximately 71% to 74%. This pattern is expected because vaccinations were introduced later in the pandemic. However, the data itself appears delayed. UK vaccinations began towards the end of 2020, but the data starts from the end of 2021.
- Mobility indices (such as Apple walking mobility and Citymapper journeys) also exhibit relatively high missing percentages (approximately 28% and 37%, respectively).
- Variables related to COVID testing and surveillance (PCR and antibody tests) have moderate missing percentages, typically ranging from 7% to 14%.
- Critical pandemic indicators such as new cases, hospital admissions, and COVID-19 deaths have relatively low missing percentages.
- The proportion of missing data increases over time, with later observations showing higher rates of missingness.

Table 2: Summary of Missing Data per Variable

Variable	Missing Count	Missing Percentage (%)
Date	0	0.00
Excess mortality	8	0.92
Schools	0	0.00
Face masks	0	0.00
Lockdown severity	0	0.00
Majority COVID-19 variant	5	0.58
Flights 7-day moving average	0	0.00
OpenTable restaurant bookings London index	144	16.63
Google homeworking Greater London mobility index	39	4.50
Google workplace Greater London mobility index	39	4.50
Apple walking London mobility index	247	28.52

Variable	Missing Count	Missing Percentage (%)
Google parks Greater London mobility index	39	4.50
Google retail recreation Greater London mobility index	39	4.50
Google grocery pharmacy Greater London mobility index	39	4.50
Google transit stations mobility index	49	5.66
TfL Tube mobility index	54	6.24
TfL Bus mobility index	54	6.24
Citymapper journeys mobility index	319	36.84
Season	0	0.00
PCR tests	107	12.36
PCR tests capacity	90	10.39
Antibody tests	121	13.97
Antibody tests capacity	70	8.08
Pillar 1 NHS and UKHSA capacity	70	8.08
Pillar 2 UK Government capacity	69	7.97
Pillar 3 Antibody capacity	120	13.86
Pillar 4 Surveillance capacity	70	8.08
Pillar 1 NHS and UKHSA tests	86	9.93
Pillar 2 UK Government tests	86	9.93
Pillar 3 Antibody tests	122	14.09
Pillar 4 Surveillance tests	62	7.16
Tests across all 4 Pillars	86	9.93
New cases	25	2.89
New infections	25	2.89
Reinfections	132	15.24
Hospital admissions	63	7.27
Patients in hospital	64	7.39
Patients in MVBs	85	9.82
Vaccinations total	355	40.99
Vaccinations 1st dose	355	40.99
Vaccinations 2nd dose	355	40.99
Vaccinations 3rd dose	639	73.79
First dose uptake	354	40.88
Second dose uptake	354	40.88
Third dose uptake	617	71.25
COVID-19 deaths on certificate	10	1.15

To enable structure learning, we imputed the missing data. Because the data are time series, we used a state space model for imputation since it accounts for temporal dynamics when estimating unobserved values. It represents time series data as a system of state and observation equations. The state equation captures the evolution of the

underlying “states” of the system over time, while the observation equation relates the states to the observed data.

The Kalman filter ([11]) is a recursive algorithm used to estimate the states in a state-space model. It is an optimal estimator when the noise is Gaussian. The Kalman filter proceeds in two steps:

- Prediction: Using the state equation to predict the next state and its uncertainty.
- Update: Incorporating the observed data to correct the predicted state.

When data points are missing, the Kalman filter will use only the prediction step to estimate the missing value and skip the update step for that time point. To enable the application of this methodology to categorical data, we created dummy variables, imputed them, and then converted them back. The reversion (from dummy variables to categorical) takes the category with the highest imputed probability as the most likely category for the missing data point. It is essential to clarify that no constant was added to this model to ensure that a dummy variable represents each level of the categorical variable. The imputation was done in R using the `na_kalman` function of the `imputeTS` package ([12]). However, the last five rows still contained missing values after imputation. This might be explained by the earlier observation that most variables show higher rates of missingness towards the end of the time series. Those last five rows were omitted from the analysis.

3.2 Data discretisation

Except for one of the econometric methods used in this study to perform structure learning, all require numeric data. Therefore, categories will be converted to numbers, so numeric data will be used for structure learning with all algorithms under consideration. However, we use the discretised dataset to later parameterise the BNs. This choice is due to the implementation restrictions in the BN software we worked with (`bnlearn`), which follows the common assumption that continuous nodes may only appear as children of discrete variables. Discretisation avoids these constraints and ensures that all nodes can be treated consistently during inference.

Given that most variables represent levels of intensity, such as indices measuring transportation usage or the number of hospitalised patients, we adopted the convention of discretising any continuous variables into three categories: low, medium, and high. We used the k-means clustering algorithm for this; specifically, the 2-means variant, implemented via the `kmeans` R function ([13]). The cluster centroids were sorted and used to determine breakpoint positions. The `cut` function is then used to categorise the original data into bins based on these breakpoints.

4 Methodology

This section outlines the methodologies applied to learn the structure of the BNs and convert them to DBNs. We first describe the econometric methods used: the Least Absolute Shrinkage and Selection Operator (LASSO), the Least Angle Regression (LAR), James-Stein Shrinkage (JS), and the Statistical Inference for Modular Networks (SIMONE). We then describe the causal ML algorithms evaluated, categorising them into constraint-based, score-based, and hybrid methods. Finally, we present the

common-knowledge graph constructed by [8], which serves as one of the benchmarks for evaluating the performance of the algorithms implemented in this study.

Assume we have a DBN with a DAG G which describes a discrete-time stochastic process $X = X_i(t); i = 1, \dots, k; t = 1, \dots, T$ taking values in R^k with k variables at t time points. If the model satisfies the following assumptions, it can be represented as a DBN:

1. The stochastic process X is first-order Markovian. This ensures that any variable at time t depends solely on the past through last period observations.
2. $\forall t > 0$, the random variables $X(t) = (X_1(t), \dots, X_k(t))$ observed at time t are conditionally independent given the random variables $X(t-1)$ at time $t-1$. This ensures that variables observed simultaneously at any given time are conditionally independent given the last period observations.
3. $X_i = (X_i(1), \dots, X_i(t))$ of any X_i cannot be written as a linear combination of X_j for any $j \neq i$. This ensures the uniqueness of G when the k variables are linearly independent.

The econometric methods model the dependence relationships in DBNs using a Vector Auto-Regressive (VAR) process. We say that a multivariate time series Y_t follows a VAR process of order p , if:

$$Y_t = c + A_1 Y_{t-1} + A_2 Y_{t-2} + \dots + A_p Y_{t-p} + \epsilon_t \quad (1)$$

Where:

- Y_t is the vector of time series variables at time t .
- c is a constant vector.
- A_i are coefficient matrices associated with the i_{th} lag of the vector of time series variables.
- ϵ_t is a vector of error terms at time t .

¹

4.1 Econometric Methods

4.1.1 Least Absolute Shrinkage and Selection Operator (LASSO)

[15] focuses on applying the LASSO for variable selection in high-dimensional graphical models. [16] first proposed the LASSO to address high-dimensional data analysis where the number of predictors far exceeds the number of observations. [15] is responsible for enabling the extension of this methodology to produce graphical models. A DAG can represent the conditional dependencies between variables, and the process in [15] can be employed to learn the structure of this graph. Focusing on a neighbourhood selection scheme using the LASSO for sparse, high-dimensional graphs, they showed that this method can recover the true graph with high probability as the sample size grows. The general idea behind using the LASSO is that real-world networks should be sparse, meaning that each variable is only directly influenced by a small number of other variables. Following the original LASSO, this is a constrained estimation procedure that tends to shrink some coefficients exactly to zero by applying an L_1

¹Please refer to [14] for further details in this methodological discussion.

norm penalty to the sum of the coefficients. Only coefficients significantly different from zero define significant dependence relationships.

We implement it in R using the lars package ([17]) in the following way:

1. We wrote a function that applies the LASSO to each variable (i.e., each column of the data frame, excluding the Date column).
2. Before fitting any model, we normalised the data using the min-max scaling approach. This ensures all variables are on a comparable scale.
3. After this, we align the predictors and target by removing a segment of observations. We remove the first p observations or last p observations, depending on whether the column will be treated as the predictor or the target at the current loop run. How p is selected will be explained in Section 6. As discussed at the beginning of this section, p is the order of the VAR process.
4. Every column that is not the target in this loop iteration will be considered a predictor. This includes the lagged target as a potential predictor.
5. For each regression, we determine the best value of the regularisation parameter. This is achieved through cross-validation, which balances model fit and complexity. Using the best regularisation parameter, we fit the model and obtain the coefficient estimates for all predictors with respect to the target.
6. If these coefficient estimates are not zero, we create a directed edge from the predictor to the target. We iterate over the coefficients and add an edge for each predictor with a non-zero coefficient, provided that adding this edge does not create a cycle.

The implementation of the LASSO in the lars package ([17]) was used with the following hyperparameter:

- **10-Fold CV**: This is the hyperparameter default and a common choice for practitioners.
- **mode = "fraction"**: This tells the function to use a fractional L_1 norm parametrisation of the solution path rather than taking discrete steps; we get a continuous parameter that can be tuned during the estimation process, resulting in a smooth, interpretable continuum of penalty strengths. This fraction instructs the algorithm on how much of the total possible L_1 norm it can utilise.
- **type = "lasso"**: This ensures the function uses the LASSO, as it can use other methods.

4.1.2 Least Angle Regression (LAR)

LAR ([18]) aims to identify a suitable subset of predictors for linear regression, particularly in situations where the number of predictors exceeds the number of observations. This allows us to model interdependencies in multivariate time series, where potential models would generate many potential predictors. Therefore, the reason this is useful for producing graphical models in a multivariate time series scenario is equivalent to the usefulness of the LASSO. In essence, they address the same problem in a slightly different way.

The estimation procedure can be described in the following steps:

1. Start with all coefficients at zero.
2. Identify the predictor most correlated with the response.

3. Move the coefficient of this predictor towards its least squares value (increasing its correlation with the evolving residual).
4. When another predictor has as much correlation with the residual, proceed in a direction equiangular between the two predictors.
5. Continue this way, adjusting predictors based on their correlations with the residuals.

The relationship between this method and DAGs is no different from the previous method. Just like the LASSO, this method will return a sparse DAG. This is because both methodologies share the principle that when there are many potential causes, we should expect only a small number to have a significant influence on other variables. We also implement this method using the `lars` package ([17]) in R. The logic behind the implementation follows the steps described for the LASSO above. The hyperparameters need to be adjusted to `type = "lar"`.

4.1.3 James-Stein Shrinkage (JS)

[19] introduces a simple algorithm to transform correlation networks (which are undirected) into DAGs, which can imply causal relationships. The algorithm proposed approximates the full search over all possible DAGs based on the idea that in a causal network, when two variables are correlated, once the influence of all other nodes on these two nodes is removed (partial correlation), their direct link can be directed according to a given order. The direction of the influence is determined by the time order; this means the lagged variable must precede the response variable in time. In time series analysis, partial correlation can help understand direct relationships between two different time series by controlling for the influence of other series. This is particularly useful in our scenario of multivariate time series; isolating the effect of individual variables is critical. This is implemented in R as an efficient estimator of the covariance matrix, which can be obtained by allowing the estimated correlation coefficients to shrink towards zero and their estimated variance to approach its median. The package that enables this implementation in R is GeneNet [20]. The following are the hyperparameters for this method:

- **method = "dynamic"**: The choice "static" (which is the default) cannot factor in temporal dependencies.
- **cutoff.ggm = 0.05**: It helps filter out non-significant connections between nodes. We choose the standard 5% significance level.
- We retain the default settings, which involve using the Student's t-test to compute p-values for each partial correlation. The Student's t-test is a classical, exact test under normality; it is designed for situations where the sample size is not huge, as in this study. We cannot change the test for different variables in the process, so we keep this classical test for our mixed dataset.
- **method.ggm = "prob"**: This means edges are selected based on their posterior probability, which means the probability that a connection is real given the data. Probability-based filtering is more robust because it incorporates significance testing, rather than simply setting a threshold based on correlation values.

4.1.4 Statistical Inference for Modular Networks (SIMONE)

SIMONE ([21]) proposes a statistical framework (and its implementation in R) for inferring modules in networks. These modules or clusters tend to be characterised by dense connections among nodes within the same cluster and fewer connections between nodes in different clusters.

Using a probabilistic model, it essentially captures the likelihood of connections between nodes based on their module memberships. This approach also incorporates a form of regularisation to discourage overly complex modules. To find the most probable modules, they proposed an optimisation procedure that considers the regularisation to maximise the model’s fit to the observed data. They tested their proposed methodology on both simulated and real-world data. It effectively recovered the true modules in simulated cases but was less successful in real-world data, where it could only reveal meaningful modules.

The R implementation of SIMONE has the following hyperparameters:

- **clusters.crit = “BIC”**: This means SIMONE will pick the network structure optimising the BIC Score, defined in Section 5. We consider this hyperparameter choice to be appropriate on the basis that this is what the score-based structure-learning algorithms, which we describe later, also optimise.
- **clustering = TRUE**: SIMONE will find nodes that share similar connections, and use that information to guide the estimation of the network structure. This hyperparameter choice is crucial for time-series data, as there are likely more variables that interact over time. Setting this hyperparameter to true means that variables like mobility and hospital burden, which become modular over time, can be modelled appropriately, leading to better regularisation and interpretability in the network.
- **type = “time-course”**: This hyperparameter is the basis of our analysis; it is where we tell SIMONE to find a network structure using a VAR process. It is the setting specifically designed for time-series data in this method.

4.1.5 Model Averaging

Above, we discussed the four different econometric methods employed to learn the structures of DBNs. Structures learnt by different methods tend to be highly inconsistent across different methods. To address this issue, we also perform model averaging on the four graphs learnt by the econometric methods to obtain an overall structure. The model-averaging output will be considered in the analysis alongside the four graphs learnt independently by each econometric method. The process employed for model averaging follows the same employed in [22], and can be described as follows:

1. Rank the edges according to the times they appear in the learnt graphs (out of four).
2. Add the edges to the overall graph following the ranking system.
3. A hyperparameter is required to specify the number of times an edge must appear across the given estimated structures (four, in this case), for it to be retained. To determine this cut-off, we optimise the BIC score (described in Section 5) across the averaged structures. That is, we evaluate each possible cut-off value

(i.e. retaining edges that appear in at least one, two, three, or all four structures), and select the value that maximises the BIC score.

4.2 Causal ML algorithms

Structure learning is an unsupervised learning process. Its traditional version is mainly based on combinatorial optimisation, where most algorithms aim to find a discrete-valued adjacency matrix. This matrix represents the presence (and their orientation) or absence of edges.

Each of the three classes of learning described in Section 1 is accompanied by its assumptions, merits, and limitations. There is no consensus regarding the preferred or appropriate class. Moreover, even algorithms within the same class of learning often produce widely different graphs. This phenomenon can be attributed, in part, to the fact that many algorithms operate on dissimilar assumptions about the input data and rely on distinct objective functions. Most of the considered objective functions are score-equivalent, yielding the same score for graphical structures belonging to the same Markov equivalence class. This characteristic implies that not all directed relationships can be recovered from observational data.

Algorithms that generate a unique DAG structure utilise objective functions that are not score-equivalent, or merely generate a random DAG from the highest-scoring equivalence class. This equivalence class is depicted by a Completed Partially Directed Acyclic Graph (CPDAG), which includes undirected edges (in addition to directed ones) that cannot be orientated from observational data alone. When faced with this issue in this study, we will use the `cextend` command from `bnlearn` ([23]) in R, which offers a consistent extension from CPDAGs to DAGs.

The algorithms used in this study are:

- PC-Stable [24]: is a constraint-based PC-derived algorithm [25]. It starts from a fully connected undirected graph, checks whether each pair of variables is conditionally independent, and removes the edge connecting them if they are. When these tests are finished, the algorithm will attempt to orientate the remaining edges.
- Grow-Shrink (GS) [26]: a constraint-based algorithm that identifies the minimal set of nodes that makes a node independent of the rest of the network to construct the network structure. This minimal set is known as a Markov Blanket. These are used to identify the neighbours (parents and children) of each node and the parents of the children. This is used to incrementally identify edges to represent dependencies amongst the variables in the data.
- Incremental Association Markov Blanket (IAMB) [27]: a modified version of the GS algorithm incorporating a two-step procedure consisting of growth and pruning phases of the Markov Blanket. This pruning phase enables a more efficient identification of the Markov blanket for each variable.
- Fast-IAMB [28]: an improved version of IAMB that aims to further improve efficiency by reducing the number of conditional independence tests.
- Interleaved Incremental Association Markov Blanket (Inter-IAMB) [27]: unlike other variants of IAMB, it uses forward-stepwise selection, which helps to improve the accuracy of the Markov blanket candidate set for each node.

- IAMB with False Discovery Rate (IAMB-FDR) ([29]): incorporates FDR in the variable selection process to reduce the number of false positives.
- H2PC [30]: a hybrid algorithm that first learns local structures around variables and then uses HC to learn the structure.
- 2-phase Restricted Maximisation (RSMAX2) [31]: identifies a small set of candidate parent variables for each target variable based on independence tests. This reduces the space of potential graphs that have to be searched.
- Hill-Climbing (HC) [32]: a score-based algorithm that begins with an empty graph and proceeds to add, remove or re-orientate edges, aiming to maximise an objective function. Only a local maximum will likely be found.
- Max-Min Hill-Climbing (MMHC) [33]: a hybrid algorithm that starts by constraining the set of parents for each node and then applies HC to find the optimal structure in the reduced search space.
- Tabu search [32]: unlike HC, Tabu - which is also score-based - sometimes makes changes that reduce the objective score, in an attempt to improve upon a local maximum solution.

The constraint-based and hybrid algorithms require the user to input the statistical test that will be used to assess conditional independence between variables. The test selected is “mi-g-sh”. According to bnlearn ([23]), this test is a shrinkage estimator based on the James-Stein estimator for mutual information. The significance level was left at the standard 0.05. The score-based and hybrid algorithms require the user to input a score that evaluates the quality of the structure learnt. The score selected is “ebic-g”. According to bnlearn ([23]), “ebic-g” extends the BIC score to add a second penalty penalising dense networks.

Both the test and score selected follow the principle of penalising dense networks. This seems a fair way to compare these methods with the econometric methods used in this study, which also employ shrinkage. As with previous relevant studies ([8],[22]), all other hyperparameters were used with their default settings. It remains unclear in the literature how to systematically compare results across different types of algorithms with varying kinds of hyperparameters. Given the extensive number of algorithms, we invite interested readers to check the default hyperparameters in [23].

4.3 Knowledge Graph

In Figure 1 below, you will find a visual representation of the knowledge graph assumed in this study. Some variables were grouped to simplify the visual:

- The 12 mobility indexes in Table 1 have been grouped as Mobility Indexes.
- The 13 variables related to tests in Table 1 have been grouped as Tests.

For a detailed explanation of how the knowledge graph was built, please refer to [8]. However, some variables were not included in the knowledge graph because we use more variables than [8], and the logic of how to integrate them was not straightforward. Specifically, :

- The date these observations were recorded.
- Those related to the number of vaccines administered daily.
- Only *Tests across all 4 Pillars* was included. The further relations between capacities and tests will be for the algorithms to discover.

The knowledge graph used in this study is based on the one described in [8], and reflects the relationship between variables relevant to the COVID-19 pandemic. It was selected for this study due to its relevance and illustrative value in demonstrating our methodology. [8] clarifies the issues they faced in modelling feedback loops, and this paper builds on the static relationships as defined in that study and extends them to temporal relationships. Figure 1 presents the knowledge graph used in this study, respecting the principles as defined in [8]. The starting point of this dynamic process is the pandemic, with infection and hospitalisation rates rising before government policies are implemented.

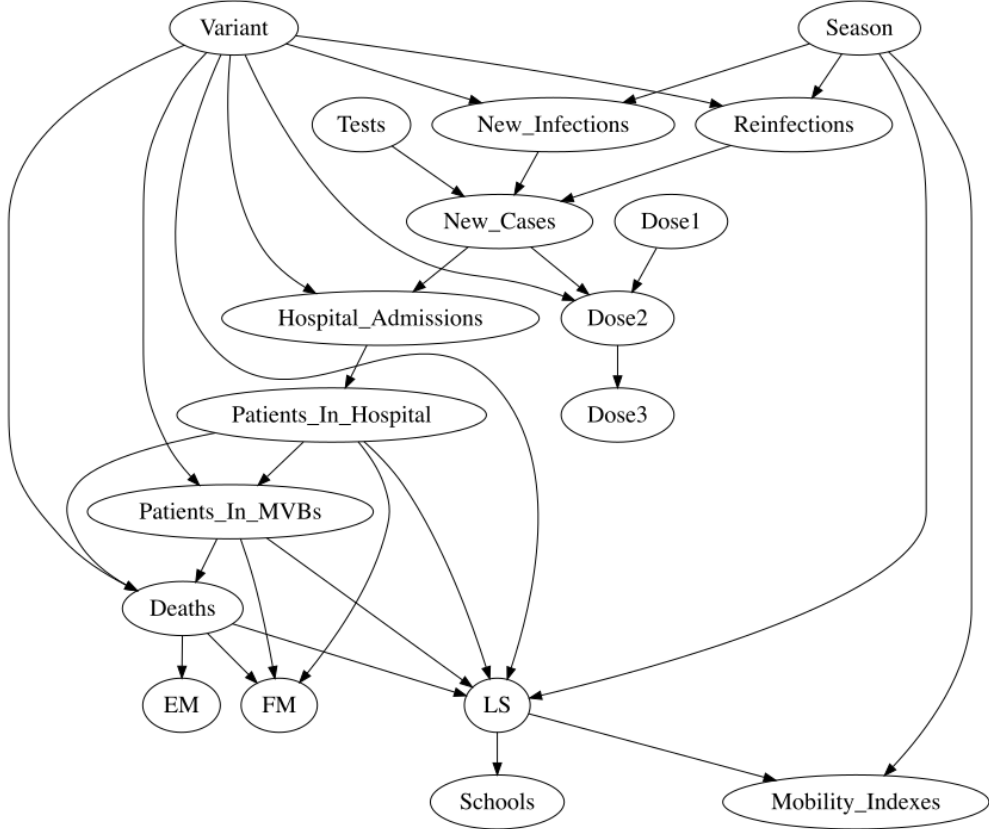


Fig. 1: The knowledge graph constructed for this study based on [8].

5 Evaluation

After running the econometric and causal ML algorithms using their respective libraries, we convert the resulting DAGs they produced into BN models using the bnlearn library ([23]). Since all of them produce a DAG structure, this conversion was

straightforward. To extend these models into DBNs, we augment the dataset with lagged versions of the variables. The output of each algorithm is then analysed through five distinct evaluation methods. These are:

- Investigating the similarities between the learnt graphs and the knowledge graph using the Structural Hamming Distance (SHD) score, which quantifies the disparities between two graphs ([33]).
- The number of free parameters, which represents the number of additional parameters generated by each edge added to the graph. This is a commonly employed metric as an indication of graph complexity.
- The number of edges indicates, reflecting graph density.
- The model selection score, BIC. We use the `bnlearn` implementation by [34], defined as:

$$BIC(G, D) = \sum_{i=1}^p [\log Pr(X_i | \prod_{X_i} X_i) - \frac{|\Theta_{X_i}|}{2} \log n] \quad (2)$$

where G denotes the graph, D the data, X_i the nodes, \prod_{X_i} the parents of node X_i , $|\Theta_{X_i}|$ the number of free parameters in the conditional probability table, and n the sample size.

- The log-likelihood (LL) is a measure of how well the generated graphs fit the data.

Assessing the benefits and limitations of the learnt structures to support policy decisions is more complex than assessing the structure alone. One way to validate them is to compare their predicted policy effects with the observed outcomes of those policies. Evaluating COVID-19 policies is particularly challenging due to the lack of consensus on the effect sizes, but there is a consensus on the direction of the effect. For example, it is inevitable that lockdowns reduce, rather than increase, infection rates. The learnt structures enable us to simulate various policy scenarios and determine which interventions, particularly those aimed at reducing social interactions, are most effective in lowering infection rates. If our structures consistently conclude that limiting interactions reduces virus transmission, for example, this would support their reliability for informing future policy decisions. Specifically, we will evaluate the ability of the generated structures in the following way:

- The number of causal effects that are identifiable by the structure. There are twelve variables related to population interactions ², and three variables related to infection rate ³. Therefore, each structure generated by the algorithms could be used to identify up to 36 (i.e., 3×12) causal effects.
- The number of times the causal effects identified have the direction of effect that the knowledge would predict; i.e., whether the effect increases or decreases. This means that we will count the times that higher limits (or, equivalently, reductions) on interactions imply reductions in infection rates.

²These are Flights (7-day moving average), OpenTable restaurant bookings (London) index, Google homeworking (Greater London) mobility index, Google workplace (Greater London) mobility index, Apple walking (London) mobility index, Google parks (Greater London) mobility index, Google retail & recreation (Greater London) mobility index, Google grocery & pharmacy (Greater London) mobility index, Google transit stations mobility index, TfL Tube mobility index, TfL Bus mobility index, Citymapper journeys mobility index

³New cases, New infections, Reinfections

6 VAR specification and Diagnostic Tests

The first part of this section describes how the order of the VAR process is estimated; i.e., the time-series process. Then, we analyse the normality of residuals of the VAR model and test for serial correlation. We discuss the impact of these traditional assumptions in our analysis. These diagnostic checks are essential for understanding the reliability of the estimation process and for determining what valid inferences we can make from the VAR model.

6.1 Optimal VAR model order

We used the VARselect function from the vars package in R ([35]) to select the optimal VAR process order p based on the following criteria:

- Akaike Information Criterion (AIC) ([36]) rewards goodness of fit but also includes a penalty for the number of parameters to avoid overfitting.
- Schwarz Criterion (SC) or Bayesian Information Criterion (BIC) ([37]) penalises the number of parameters more heavily than AIC, often leading to more parsimonious models.
- Hannan-Quinn Information Criterion (HQ) ([38]) is a compromise between AIC and BIC, with a penalty term intermediate in magnitude between the two.
- Final Prediction Error (FPE) ([39]) is based on the predicted one-step-ahead prediction error.

For each model order from 1 to the maximum selected, the VARselect function fits a VAR model and calculates these information criteria. The order that minimises each criterion is then chosen. Initially, we did not set a maximum lag. However, Table 3 shows that a maximum lag of 17 was used. We discuss this below.

Each criterion has strengths and weaknesses, and there is no correct choice for all circumstances. Results are expected to be compared across criteria, and additional diagnostic tools and domain knowledge will be used to finalise the model order selection.

Table 3: Lag selection criteria

Criterion	Formula	Optimal number of lags
AIC	$-2\ln(L) + 2k$	17
SC	$-2\ln(L) + k\ln(n)$	1
HQ	$-2\ln(L) + 2k\ln\ln(n)$	17
FPE	$\frac{\hat{\sigma}_p^2}{n} \frac{n+p+1}{n-p-1}$	17

where L is the likelihood of the model, k is the number of estimated parameters, n is the number of observations, and $\hat{\sigma}_p^2$ is the estimated variance of the error term.

AIC, HQ, and FPE find the optimal order of the VAR model at 17 lags, while SC's optimal order is one lag. We ran VARselect with a maximum possible order of more than 17 on the COVID-19 case study (meaning we ran VARselect with a maximum

possible order of 18, 19, and so forth), and all of the metrics started choosing the maximum possible lag as the optimal lag (meaning all the metrics started choosing model orders of 18, 19 and so forth). This is a problem, since this parameter explosion would make the estimation of this VAR model unreliable or intractable. Figure 2 helps us to visualise the issue. There are three possible explanations for this phenomenon:

- The data has structural breaks and outliers. The VAR model will attempt to compensate for this by using additional lags.
- We must recognise the possibility of omitted variables, such as latent confounders and other dynamics not properly captured in our dataset. The model will attempt to compensate by selecting more lags.
- To some extent, these metrics focus on performance on training data. Therefore, more complexity will be good for this purpose, but not for performance in out-of-sample data.

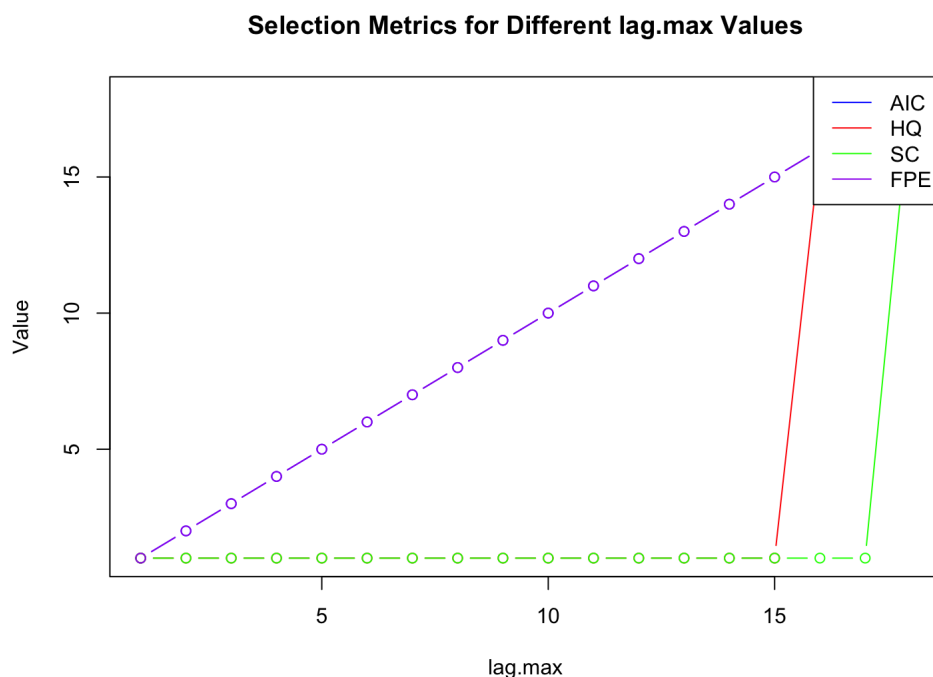


Fig. 2: The optimal VAR order for each metric for each possible maximum model order.

On this basis, we proceeded with a VAR model of order one (i.e., with one lag). This would make the model more parsimonious, especially in the presence of 46 variables and 866 observations. The more lagged variables we create from the original variables, the more the number of variables will converge to the sample size. Given that generating the first lag of all our variables gives us 92 potential variables to be included

in a model, we assume $VAR(1)$ to be the optimal choice. While this might seem odd in the context of supporting policy decisions in the COVID-19 pandemic, looking at the Partial Autocorrelation Function (PACF) of *New Infections* shows a significant positive partial autocorrelation at lag 1. Although further lags remain significant, the decrease in the size of the PACF is considerable after lag 1, which measures the correlation between the current observation and previous lagged observations, controlling for the lags in between them. For lag 1, the PACF is equal to the Autocorrelation Function. This provides a better understanding that, although we might expect the impact of policies to take longer than one period, the last period holds most of the information we need for this analysis. This makes sense since changes will be gradual, and the number of new infections today will be closely related to the number of new infections yesterday. The PACF for *New Infections* is presented in Figure 3 below.

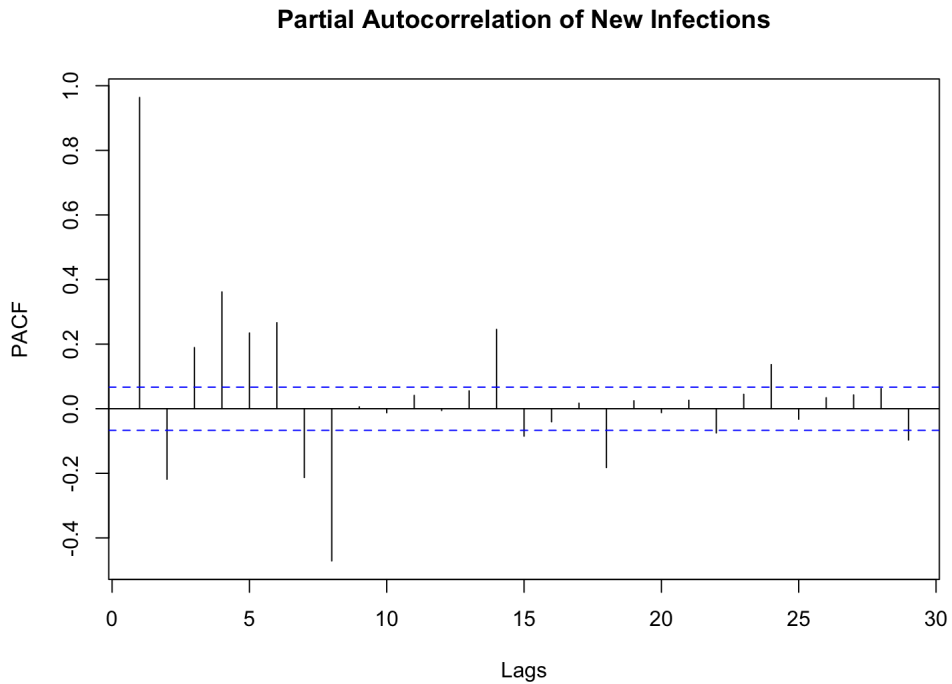


Fig. 3: The Partial Autocorrelation of New Infections.

6.2 Normality of residuals

The Jarque-Bera test ([40]) is a goodness-of-fit test that relies on the assumption that, under the null hypothesis, both the skewness and kurtosis of the population from which the sample is drawn are those of a normal distribution (i.e., skewness = 0 and excess kurtosis = 0). The test statistic JB is computed as:

$$JB = \frac{n}{6} \left(S^2 + \frac{1}{4}(K - 3)^2 \right) \quad (3)$$

Where n is the sample size, S is the sample skewness, and K is the sample kurtosis. If the sample skewness and excess kurtosis significantly deviate from zero, there is evidence to reject the null hypothesis in favor of the alternative that the data do not come from a normally distributed population. In R, this is implemented via the `jarque.bera.test` function of the moments package ([41]). These results are presented in Table 4.

Table 4: Jarque-Bera Tests Results

Variable	X-squared	df	p-value
EM	57375	2	< 0.001
Schools	1886013	2	< 0.001
FM	2292604	2	< 0.001
LS	340414	2	< 0.001
Variant	1751490	2	< 0.001
Flights	869.26	2	< 0.001
Restaurant	18932	2	< 0.001
Homeworking	140.54	2	< 0.001
Workplace	221.52	2	< 0.001
Walking	1705.8	2	< 0.001
Parks	327.34	2	< 0.001
Retail & recreation	8459.3	2	< 0.001
Grocery & Pharmacy	21820	2	< 0.001
Transit	957.71	2	< 0.001
Tube	8336.4	2	< 0.001
Bus	1097.3	2	< 0.001
Journeys	30853	2	< 0.001
Season	391019	2	< 0.001
PCR tests	315.31	2	< 0.001
PCR tests capacity	551227	2	< 0.001
Antibody tests	25300	2	< 0.001
Antibody tests capacity	1140233	2	< 0.001
Pillar 1 capacity	3207734	2	< 0.001
Pillar 2 capacity	601332	2	< 0.001
Pillar 3 capacity	3969140	2	< 0.001
Pillar 4 capacity	2101.4	2	< 0.001
Pillar 1 tests	79.16	2	< 0.001
Pillar 2 tests	2486.6	2	< 0.001
Pillar 3 tests	33161	2	< 0.001
Pillar 4 tests	1126.1	2	< 0.001
Tests across all 4 Pillars	2354.6	2	< 0.001
New cases	29868	2	< 0.001

Table 4: Jarque-Bera Tests Results (continued)

Variable	X-squared	df	p-value
New infections	28258	2	< 0.001
Reinfections	29486	2	< 0.001
Hospital admissions	1181.2	2	< 0.001
Patients in hospital	454.62	2	< 0.001
COVID Patients in MVBs	231.69	2	< 0.001
Vaccinations (total)	1672.3	2	< 0.001
Vaccinations (1st dose)	25080	2	< 0.001
Vaccinations (2nd dose)	13233	2	< 0.001
Vaccinations (3rd dose)	39094	2	< 0.001
1st dose uptake	22.49	2	< 0.001
2nd dose uptake	53.617	2	< 0.001
3rd dose uptake	180116	2	< 0.001
COVID-19 deaths on certificate	1364.9	2	< 0.001

As shown in Table 4, the p-values for all the series are very close to zero, leading to the rejection of the null hypothesis in all cases. This suggests that the residuals of all the variables in our VAR model do not follow a normal distribution, and this violates the assumption of the VAR process in that the error is normally distributed. However, the properties of Ordinary Least Squares (OLS) used to estimate the VAR model, on consistency and unbiasedness, do not rely on the normality assumption. This is sufficient for this study, as the existence of edges in the DAGs is derived from the coefficients of the VAR model. Since we have consistency, we know that as the sample size tends to infinity, the estimator of the coefficients converges to the true value of the parameters. Since the estimators are unbiased, we know that, on average, the estimators do not overestimate or underestimate the true values of the parameters. Therefore, we consider the coefficients obtained to be reliable. However, in the case of the JS method, failing normality implies that the Student's t-test no longer holds, and this is a limitation where we should expect JS to produce some false positive edges.

6.3 Test for serial correlation

The Breusch-Godfrey test ([42] and [43]) is used to detect autocorrelation in the residuals of a regression model. The following is a description of the process of the Breusch-Godfrey Test:

- a. Estimate the model and obtain the residuals:

$$Y_t = \beta_0 + \beta_1 X_{1,t} + \dots + \beta_k X_{k,t} + u_t$$

b. Run the auxiliary regression:

$$u_t = \alpha_0 + \alpha_1 X_{1,t} + \dots + \alpha_k X_{k,t} + \delta_1 u_{t-1} + \dots + \delta_p u_{t-p} + v_t$$

where p represents the number of lags tested for autocorrelation.

c. Compute the LM statistic:

$$LM = T \cdot R^2$$

where T denotes the sample size and R^2 represents the coefficient of determination from the auxiliary regression. Under the null hypothesis of no autocorrelation, this statistic follows a chi-squared distribution with p degrees of freedom.

In R, this test is implemented equation-by-equation of the VAR model as follows:

- a. Select an equation from the VAR.
- b. Fit this equation using the `lm` function to extract the residuals (errors).
- c. Apply the Breusch-Godfrey test via the `bgtest` function of the `lmtest` library ([44]) to the fitted model.

The loop automates this process for each variable in the VAR model, testing each one for serial correlation. The results of this test are presented in Table 5.

Table 5: Breusch-Godfrey Test Results

Test	LM test	df	p-value
EM	3.253	1	0.007
Schools	0.341	1	0.559
FM	0.061	1	0.806
LS	0.002	1	0.962
Variant	0.898	1	0.343
Flights	288.03	1	< 0.001
Restaurant	6.837	1	0.009
Homeworking	32.444	1	< 0.001
Workplace	28.705	1	< 0.001
Walking	22.703	1	< 0.001
Parks	3.882	1	0.049
Retail & recreation	0.099	1	0.753
Grocery & Pharmacy	0.135	1	0.713
Transit	1.096	1	0.295
Tube	2.962	1	0.085
Bus	15.658	1	< 0.001
Journeys	0.002	1	0.963
Season	0.507	1	0.476
PCR tests	2.548	1	0.11
PCR tests capacity	1.871	1	0.171
Antibody tests	37.832	1	< 0.001
Antibody tests capacity	2.102	1	0.147

Table 5: Breusch-Godfrey Test Results (continued)

Test	LM test	df	p-value
Pillar 1 capacity	1.362	1	0.243
Pillar 2 capacity	1.529	1	0.216
Pillar 3 capacity	1.144	1	0.285
Pillar 4 capacity	24.712	1	< 0.001
Pillar 1 tests	19.349	1	< 0.001
Pillar 2 tests	0.01	1	0.92
Pillar 3 tests	167.59	1	< 0.001
Pillar 4 tests	2.836	1	0.092
Tests across all 4 Pillars	0.008	1	0.93
New cases	119.92	1	< 0.001
New infections	112.91	1	< 0.001
Reinfections	142.35	1	< 0.001
Hospital admissions	0.085	1	0.771
Patients in hospital	8.496	1	0.004
COVID Patients in MVBs	74.709	1	< 0.001
Vaccinations (total)	3.656	1	0.056
Vaccinations (1st dose)	0.386	1	0.534
Vaccinations (2nd dose)	17.615	1	< 0.001
Vaccinations (3rd dose)	3.192	1	0.074
1st dose uptake	138.42	1	< 0.001
2nd dose uptake	261.06	1	< 0.001
3rd dose uptake	6.466	1	0.011
COVID-19 deaths on certificate	47.388	1	< 0.001

If the p-value is less than the significance level of 0.05, there is evidence of serial correlation in the residuals. These results suggest that the assumption about the behaviour of the residuals in a VAR process is violated. However, the estimate of the coefficients remains unbiased, which is adequate for the edge selection approach, which is based on coefficient magnitude. Still, this is acknowledged as a limitation.

7 Results

The first subsection focuses on structure learning and compares the learnt structures to the knowledge graph, as well as metrics that describe the fit and complexity of the learnt structures. The subsequent subsection discusses policy evaluation, focusing on understanding the quality of the structures learnt concerning their application in decision-making.

7.1 Graphical and modelling metrics

The numerical results are summarised in Table 6. The model-averaged structure (“Average”) includes any edge that appears in at least two of the four algorithms.⁴ This approach increases the number of edges, and does not achieve the best BIC score amongst the econometric methods; SIMONE tops BIC as well as the LL score.⁵

SHD counts the number of changes needed to turn a learnt graph into the knowledge graph. These changes involve adding, removing, or reorientating an edge. The results show high SHD values for many algorithms, similar to the findings of [8]. For example, the structure learnt by LASSO contains 161 edges, yet its SHD relative to the knowledge graph is 246. This suggests that there is limited overlap between the LASSO-derived structure and the knowledge graph; essentially, to convert the LASSO graph into the common-knowledge structure, one would have to remove most of LASSO’s edges and then add most edges from the knowledge graph. A strong conclusion that can be derived from these results is that the knowledge graph does not agree with the learnt graphs. However, Figure 4 shows there are considerable differences in the graphs learnt by the econometric methods as well.

The number of free parameters varies noticeably across the algorithms, as expected given their substantially different learnt structures. Although the averaged model is more complex than SIMONE, its fit is weaker. Within the econometric set, SIMONE offers the best fit. The average model only improves over LASSO, LAR, and JS, but does not surpass SIMONE. At the lower-performing end in Table 6 is the knowledge structure with a relatively weak LL score. This is not unexpected, as the learning algorithms explicitly optimise fit to the data, whereas the knowledge graph was not derived from data fitting.

The causal ML algorithms show SHD values that are mostly lower than those of the econometric methods, except for the two score-based algorithms HC and TABU. This is due to these score-based methods producing considerably more edges than the other algorithms, leading to substantially more complex structures than any of the other methods tested in this study, but with considerably better LL scores too. Conversely, the constraint-based methods learnt relatively sparse graphs, yet still attained competitive BIC and reasonably good LL scores.

The econometric methods are at a disadvantage in terms of BIC and LL scores, and this might be because they inherently enforce temporal constraints. In our VAR(1) specification, each node at time t may only have parents at time $t - 1$, so the resulting DBNs contain only past-to-present edges. This consideration becomes crucial in the next section, where we discuss the utility of these methods in informing policy decisions, showing that if an algorithm cannot discern the correct temporal order of relationships, its value for policy analysis is limited.

⁴The LASSO and LAR could not be parametrised because of the sizes of CPT that generated a bnlearn error. Therefore, only coefficients greater than 0.4 instead of 0 were considered. The model-averaged structure could only consider adding edges that appear in at least two of the structures for the same reason.

⁵It is important to state that after using the `cextend` command from bnlearn ([23]) in R, GS edges could not be oriented to construct a DAG. Therefore, no results from GS are shown.

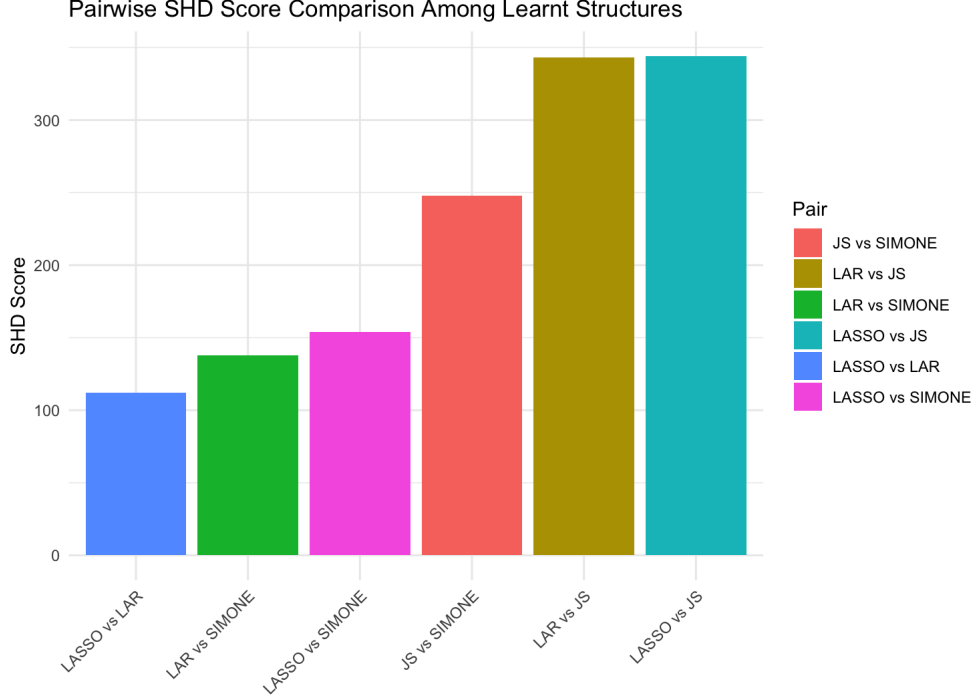


Fig. 4: SHD comparison amongst the learnt econometric structures. The figure was produced using ggplot2 ([45]).

7.2 Policy Evaluation

Simulating interventions in CBNs is equivalent to manipulating a variable in the model. In this study, this is equivalent to, for example, a policy intervention aimed at reducing one of the mobility indices and estimating the impact of this action on future cases of COVID-19. We use Pearl’s [7] do-operator to simulate interventions for causal effect estimation, where $P(Y|do(X = x))$ represents the probability of observing Y if we manipulate X and set it to the state x . We use the R package `causaleffect` ([46]) to compute causal effects, which implements [47] and [48], and implement this using `bnlearn` ([23]) and its `cpquery` function ([23]), which is based on Monte Carlo particle filters.

Since the data is discretised into three different states for continuous variables, we compute the Average Causal Effect (ACE) as follows:

$$\frac{1}{2} [(P(Y|do(X = 2)) - P(Y|do(X = 3))) + (P(Y|do(X = 1)) - P(Y|do(X = 3)))] \quad (4)$$

The ACE represents the average change in the probability of an outcome (Y) as treatment (X) changes from a baseline state, and averages the effects across the

Table 6: Structure learning results

Algorithms	SHD	No. of free parameters	No. of Edges	BIC	LL
LASSO	246	258	161	-40213	-39341
LAR	246	263	163	-39683	-38795
JS	246	725	195	-53467	-51017
SIMONE	151	109	66	-36914	-36546
Average	209	238	126	-39435	-38631
Knowledge-based	0	407	91	-61946	-60571
PC-Stable	147	101	57	-35192	-34851
GS	NA	NA	NA	NA	NA
IAMB	155	103	65	-35103	-34755
Fast-IAMB	153	101	63	-34851	-35192
Inter-IAMB	155	103	65	-35103	-34755
IAMB-FDR	148	101	58	-35192	-34851
RSMAX2	103	189	13	-65153	-64514
MMHC	108	197	18	-62878	-62212
H2PC	102	189	12	-65229	-64591
HC	738	1662	697	-24749	-19134
TABU	740	1660	699	-24733	-19124

transitions of the treatment variable. When we compute $P(Y | \text{do}(X = x))$, X refers to the value of the intervention variable at time $t - 1$ and Y to the outcome at time t . The ACEs reported below, therefore, represent the average one-step-ahead.

Equation (4) calculates the ACE of lowering X from a baseline set to 3, where 3 identifies the state associated with the highest values these variables can take. Here, X represents the variables related to population interactions and Y represents the variables associated with the infection rate defined in Section 5. X will be set to 3 because we want to understand if changing X from a high level of population interactions to low levels of population interactions decreases the likelihood of high levels of Y .

Table 7 below presents the results related to the evaluation metrics of the number of causal effects identified and the number of times the direction of the effect matches that of common knowledge. Table 8 presents the average causal effects that are identified and match the direction of knowledge.

As shown in Table 7, the only algorithms that identify a substantial number of causal effects are HC and TABU (27 effects each), with 14 and 12 of those effects respectively pointing in the direction suggested by common knowledge of the pandemic (e.g., reduced population interactions imply fewer COVID-19 cases). JS identifies 2 effects, but both match the expected direction of the effect. HC and TABU yield the most identifiable effects, explained by the denser graphs they produced, and this trade-off between identifiability and model sparsity warrants further investigation. However, unlike the econometric methods, these causal-ML algorithms were not constrained to respect the chronological order of the time series. Although the learnt graphs are acyclic in the static sense, they might display edges that are incompatible with the underlying temporal order. Therefore, Table 8 reports Average Causal Effects (ACEs) only for those effects that satisfy all of the following: (i) they are identifiable in the learnt graph, (ii) their direction is consistent with prior/common knowledge, and (iii)

they are obtained from a DBN derived from an econometric method that enforces past-to-present temporal structure (here, the JS-based model).

Under these criteria, two such interventions appear in our dataset: lowering the Citymapper journeys index and lowering OpenTable restaurant activity, each of which reduces the probability of high reinfections. Interestingly, TABU and HC also identified these effects. The effects are similar in size to those of JS. For Citymapper journeys, they stand at -0.02 for TABU and -0.01 for HC. For OpenTable restaurant activity, they stand at -0.003 for TABU and -0.001 for HC. We view this as a robustness check.

These effects are modest in magnitude but align with the expected mechanism, which suggests that reduced out-of-home mobility and indoor social activity lower transmission risk. However, there appears to be consistency across algorithms regarding the effects JS identified. This suggests that amongst the COVID-19 interventions evaluated, limiting these interactions are the most effective at reducing infection rates in the UK data. This conclusion is not easy to unravel. A crucial question here, for example, is why they are undertaking these journeys. There is evidence that although households accounted for 6% of the contacts, they were responsible for 40% of COVID-19 transmissions ([49]). Additionally, individuals at greater distances require longer exposures to contract contagion ([49]). This, paired with the OpenTable restaurant results, suggests that travel involving close contact with familiar people increases the risk of contagion, since such interactions are more likely to occur in close proximity.

Table 7: Policy evaluation results

Algorithms	No. of causal effects identified	No. of times direction matches knowledge
LASSO	0	0
JS	2	2
SIMONE	0	0
LAR	0	0
Average	0	0
Knowledge-based	0	0
PC-Stable	0	0
GS	NA	NA
IAMB	0	0
Fast-IAMB	0	0
Inter-IAMB	0	0
IAMB-FDR	0	0
RSMAX2	0	0
MMHC	0	0
H2PC	0	0
HC	27	14
TABU	27	12

8 Conclusion

This study examines how causal relationships, rather than mere associations, can be identified or assumed and used for policy evaluation. It compares econometric

Table 8: Average causal effects (ACEs) of selected mobility interventions on high reinfections, estimated from the JS-based DBN. Only effects that are (i) identifiable from the learnt graph and (ii) directionally consistent with common knowledge are reported.

Cause	Effect	Average Causal Effect
Citymapper journeys	Reinfections	-0.04
OpenTable restaurant	Reinfections	-0.003

time-series methods with causal ML approaches to assess their effectiveness in causal discovery and causal modelling. While our results show that econometric techniques offer strengths that help address the current limitations of Causal ML in time-series contexts, both approaches present trade-offs, and neither can yet be considered universally superior.

Using an evaluation strategy that includes metrics related to learning the causal structure as well as the success of these structures in computing the direction (i.e., positive or negative) of the causal effect to support policy decisions, we found that:

- There is substantial variation in the structures learnt by the econometric methods.
- Model complexity varies widely; JS is markedly more complex than LASSO/LAR, while SIMONE is comparatively sparse.
- Within the econometric methods, SIMONE achieves the best BIC and LL; the averaged model does not outperform SIMONE. The knowledge graph performs worst on BIC/LL and has the most free parameters.
- In policy evaluation, JS identifies two relevant causal effects, and both align with common knowledge. Score-based algorithms (HC, TABU) identify many more effects (27 each) but at the cost of very dense graphs and without temporal restrictions, and only a subset (14,12) aligns with the knowledge graph. Overall, evidence is mixed, not uniformly in favour of one family.
- Relative to traditional causal-ML, the econometric methods generally have higher SHD and (except SIMONE) more edges, and they underperform on BIC/LL, bearing in mind that time-order restrictions were not imposed on the traditional algorithms.
- Incorporating explicit temporal structure and modularity ideas from the econometric approaches into causal ML could reduce edges needed for identifiability and improve policy usefulness.
- Some exploration is needed on how score-based methods regularise their models, as they still produce extremely dense graphs. Perhaps the econometric methods can also offer some insights into this space.

Across methods, the clearest and most consistent policy signal concerned reducing journeys, thereby lowering the risk of reinfection. Although effect sizes from one day to the next were modest, this aligns with the mechanism that sustained, close-contact interactions drive transmission. For decision-makers, models that encode temporal precedence and penalise complexity seem more reliable for stress-testing interventions.

Limitations include non-normal errors, pockets of residual autocorrelation, and potential omitted variables point to model misspecification risks. Discretisation

(required for DBN parametrisation) may attenuate the signal, and the lack of universally imposed temporal constraints complicates head-to-head comparisons. The knowledge graph was not designed for dynamic settings, further limiting SHD interpretability.

This study’s comparison of methods produces results that could guide further work. The econometric methods failed to deal with the complexity of this dataset and the omitted variables. It is also clear that more work is needed to develop methodologies that can more accurately identify cause-and-effect relationships to inform policy decisions in time-series settings. This is made clear by the fact that while it is common knowledge that preventing human contacts prevents pandemics from spreading, many of the algorithms tested failed to detect these relationships.

Declarations

8.1 Data availability and access

The data used in this study have been submitted alongside the paper. Code, replication materials, and additional documentation are available in the accompanying GitHub repository:

<https://github.com/br1pa/econometric-vs-causal-time-series>

8.2 Competing interests

The authors declare that they have no known competing financial interests or personal relationships that could have appeared to influence the work reported in this paper.

8.3 Ethical and informed consent for data used

This article does not contain any studies with human participants or animals performed by any of the authors.

8.4 Contributions

Bruno Petru ngaro: Conceptualisation, Methodology, Software, Analysis, Writing-original draft preparation, review and editing. Anthony C. Constantinou: Writing - Review & Editing, Supervision.

References

- [1] Athey, S., Imbens, G.W.: The state of applied econometrics: Causality and policy evaluation. *Journal of Economic Perspectives* **31**(2), 3–32 (2017) <https://doi.org/10.1257/jep.31.2.3>
- [2] Pinotti, P.: Clicking on heaven’s door: The effect of immigrant legalization on crime. *American Economic Review* **107**(1), 138–68 (2017) <https://doi.org/10.1257/aer.20150355>

- [3] Kocacoban, D., Cussens, J.: Online causal structure learning in the presence of latent variables. 2019 18th IEEE International Conference On Machine Learning And Applications (ICMLA), 392–395 (2019) <https://doi.org/10.1109/ICMLA.2019.00073>
- [4] Kummerfeld, E., Danks, D.: Online learning of time-varying causal structures. In: UAI Workshop on Causal Structure Learning (2012)
- [5] Kummerfeld, E., Danks, D.: Tracking time-varying graphical structure. *Advances in neural information processing systems* **26** (2013)
- [6] Kermack, W., McKendrick, A.: Contributions to the mathematical theory of epidemics. *Proceedings of the Royal Society of London A* **115**(772), 700–721 (1927)
- [7] Pearl, J.: Causal diagrams for empirical research. *Biometrika* **82**, 669–710 (1995)
- [8] Constantinou, A., et al.: Open problems in causal structure learning: A case study of covid-19 in the uk. *Expert Systems with Applications* **234** (2023) <https://doi.org/10.1016/j.eswa.2023.121069>
- [9] Coronavirus (COVID-19): Testing in United Kingdom. The Official UK Government Website for Data and Insights on Coronavirus (COVID-19).
- [10] GOV.UK (2022d). Coronavirus (COVID-19): Healthcare in United Kingdom. The Official UK Government Website for Data and Insights on Coronavirus (COVID-19).
- [11] Kalman, R.E.: A new approach to linear filtering and prediction problems. *Journal of Basic Engineering* **82**(1) (1960) <https://doi.org/10.1115/1.3662552>
- [12] Moritz, S., Bartz-Beielstein, T.: imputeTS: Time Series Missing Value Imputation in R. *The R Journal* **9**(1), 207–218 (2017) <https://doi.org/10.32614/RJ-2017-009>
- [13] Hartigan, J.A., Wong, M.A.: Algorithm as 136: A k-means clustering algorithm. *Journal of the royal statistical society. series c (applied statistics)* **28**(1), 100–108 (1979)
- [14] Radhakrishnan, N., et al.: *Bayesian Networks in R with Applications in Systems Biology*. Springer (2013)
- [15] Meinshausen, N., Bühlmann, P.: Variable selection and high-dimensional graphs with the lasso. *Annals of Statistics* **34**, 1436–1462 (2006)
- [16] Tibshirani, R.: Regression shrinkage and selection via the lasso. *Journal of the Royal Statistical Society Series B: Statistical Methodology* **58**(1), 267–288 (1996)
- [17] Hastie, T., Efron, B.: *lars: Least angle regression, lasso and forward stagewise*

(Retrieved December, 2023)

- [18] Efron, B., *et al.*: Least angle regression. *The Annals of Statistics* **32**(2), 407–451 (2004)
- [19] Opgen-Rhein, R., Strimmer, K.: Learning causal networks from systems biology time course data: an effective model selection procedure for the vector autoregressive process. *BMC bioinformatics* **8**(2), 1–8 (2007)
- [20] Schaefer, J., *et al.*: Genenet: Modeling and inferring gene networks (Retrieved December, 2023)
- [21] Chiquet, J., *et al.*: Simone: Statistical inference for modular networks. *Bioinformatics* **25**(3), 417–418 (2009)
- [22] Petrungaro, B., Kitson, N.K., Constantinou, A.C.: Investigating potential causes of sepsis with bayesian network structure learning. *Applied Intelligence* **55**(6), 496 (2025)
- [23] Scutari, M.: Learning bayesian networks with the bnlearn R package. *Journal of Statistical Software* **35**(3), 1–22 (2010) <https://doi.org/10.18637/jss.v035.i03>
- [24] Colombo, D., *et al.*: Order-independent constraint-based causal structure learning. *J. Mach. Learn. Res.* **15**(1), 3741–3782 (2014)
- [25] Spirtes, P., *et al.*: An algorithm for fast recovery of sparse causal graphs. *Social science computer review* **9**(1), 62–72 (1991)
- [26] Margaritis, D.: Learning bayesian network model structure from data. PhD thesis, School of Computer Science, Carnegie Mellon University Pittsburgh, PA, USA (2003)
- [27] Tsamardinos, I., *et al.*: Algorithms for large scale markov blanket discovery. In: FLAIRS Conference, vol. 2, pp. 376–380 (2003). St. Augustine, FL
- [28] Yaramakala, S., *et al.*: Speculative markov blanket discovery for optimal feature selection. In: Fifth IEEE International Conference on Data Mining (ICDM’05), p. 4 (2005). IEEE
- [29] Pena, J.M.: Learning gaussian graphical models of gene networks with false discovery rate control. In: European Conference on Evolutionary Computation, Machine Learning and Data Mining in Bioinformatics, pp. 165–176 (2008). Springer
- [30] Gasse, M., *et al.*: A hybrid algorithm for bayesian network structure learning with application to multi-label learning. *Expert Systems with Applications* **41**(15), 6755–6772 (2014)

- [31] Friedman, N., et al.: Learning bayesian network structure from massive datasets: The "sparse candidate" algorithm. arXiv preprint arXiv:1301.6696 (2013)
- [32] Bouckaert, R.R.: Bayesian belief networks: from construction to inference. PhD thesis (1995)
- [33] Tsamardinos, I., *et al.*: The max-min hill-climbing bayesian network structure learning algorithm. *Machine learning* **65**, 31–78 (2006)
- [34] Scutari, M., Denis, J.-B.: *Bayesian Networks with Examples in R*, 2nd edn. Chapman and Hall, Boca Raton (2021). ISBN 978-0367366513
- [35] Pfaff, B.: Var, svar and svec models: Implementation within R package vars. *Journal of Statistical Software* **27**(4) (2008)
- [36] Akaike, H.: A new look at the statistical model identification. *IEEE transactions on automatic control* **19**(6), 716–723 (1974)
- [37] Schwarz, G.: Estimating the dimension of a model. *The annals of statistics*, 461–464 (1978)
- [38] Hannan, E.J., Quinn, B.G.: The determination of the order of an autoregression. *Journal of the Royal Statistical Society: Series B (Methodological)* **41**(2), 190–195 (1979)
- [39] Akaike, H.: Fitting autoregressive models for prediction. *Ann Inst Stat Math* **21**, 243–247 (1969) <https://doi.org/10.1007/BF02532251>
- [40] Jarque, C.M., Bera, A.K.: A test for normality of observations and regression residuals. *International Statistical Review/Revue Internationale de Statistique*, 163–172 (1987)
- [41] Komsta, L., Novomestky, F.: *Moments: Moments, Cumulants, Skewness, Kurtosis and Related Tests*. (2022). R package version 0.14.1. <https://CRAN.R-project.org/package=moments>
- [42] Godfrey, L.G.: Testing against general autoregressive and moving average error models when the regressors include lagged dependent variables. *Econometrica: Journal of the Econometric Society*, 1293–1301 (1978)
- [43] Breusch, T.S.: Testing for autocorrelation in dynamic linear models. *Australian economic papers* **17**(31), 334–355 (1978)
- [44] Zeileis, A., Hothorn, T.: Diagnostic checking in regression relationships. *R News* **2**(3), 7–10 (2002)
- [45] Wickham, H.: *Ggplot2: Elegant Graphics for Data Analysis*. Springer, New York, USA (2016). <https://ggplot2.tidyverse.org>

- [46] Tikka, S., Karvanen, J.: Identifying causal effects with the R package causaleffect. *Journal of Statistical Software* **76**(12), 1–30 (2017) <https://doi.org/10.18637/jss.v076.i12>
- [47] Shpitser, I., Pearl, J.: Identification of conditional interventional distributions. arXiv preprint arXiv:1206.6876 (2012)
- [48] Shpitser, I., Pearl, J.: Identification of joint interventional distributions in recursive semi-markovian causal models. In: *Proceedings of the National Conference on Artificial Intelligence*, vol. 21, p. 1219 (2006). Menlo Park, CA; Cambridge, MA; London; AAAI Press; MIT Press; 1999
- [49] Ferretti, L., et al.: Digital measurement of sars-cov-2 transmission risk from 7 million contacts. *Nature* (2023)